Emulsion Polymerization of Styrene with Amphiphilic Random Copolymer as Surfactant: Predominant Droplet Nucleation

Li Liu,[1,2] Xiao-Li Liu,[1] Ye Han,[1,2] Qing-Rui Chen,[1] Jing-Feng Yu,[1] Feng-Qi Liu[1]

[1]*Department of Chemistry, Jilin University, 2699 Qianjin Street, Changchun 130012, China*
[2]*Department of Chemical Engineering, Changchun University of Technology, 17 Yanan Street, Changchun 130012, China*

Received 6 September 2008; accepted 22 March 2009
DOI 10.1002/app.30483
Published online 27 May 2009 in Wiley InterScience (www.interscience.wiley.com).

ABSTRACT: Amphiphilic random copolymer consisting of monomeric units of poly (butyl acrylate) and poly (maleic acid salt) was synthesized and characterized. The emulsion polymerization kinetics of styrene stabilized by this copolymer was investigated. The influencing factors, including polymeric surfactant concentration, initiator concentration and polymerization temperature, were systematically studied. The kinetic data show that the polymerization rate (R_P) increased with the increase of the polymeric surfactant concentration ([S]) and polymerization temperature (T). At the higher [S], droplets nucleation and micelle nucleation coexisted in the polymerization system; at the lower [S], only the droplets nucleation process existed. The polymerization did not follow Smith-Ewart Case II kinetics. Dynamic light scatter and transmission electron microscope were utilized to measure the sizes and shapes of the particles, respectively. It would be speculated that a kind of large heterogeneous particles with multiple-active-sites was formed in the polymerization system. The increasing of R_P with increasing initiator concentration ([KPS]) was rapid at a medium [KPS], but the slowly increasing was observed at a lower or higher [KPS]. It was attributed to the barrier effect of the polymeric surfactant around the monomer droplets. The polymerization activation energy was 60.29 kJ/mol. © 2009 Wiley Periodicals, Inc. J Appl Polym Sci 113: 4023–4031, 2009

Key words: amphiphilic random copolymer; styrene; kinetics; emulsion polymerization; micelle

INTRODUCTION

Recently, polymeric surface-active materials as stabilizers in various aqueous emulsion polymerizations have been utilized extensively.[1–12] Compared with conventional surfactants, polymeric surfactants have relatively low critical micelle concentration (CMC) and they provide stability for emulsion by a steric repulsion force or an electrostatic repulsion effect between interacting particles. In addition, an anchoring counterpart should also exist in the stabilizer chain which anchors firmly on the surface of particles to prevent stabilizer molecules from desorption. This gives latex excellent stability against high electrolyte concentrations, freeze thaw cycling, and high shear rates. Understanding the role of this kind of polymeric surfactants in emulsion polymerizations is of particular interest.

Most of the polymeric stabilizers are amphiphilic block or graft copolymers in nature containing separate hydrophobic and hydrophilic units. A typical class of polymeric stabilizers is some amphiphilic copolymers which have polyoxyethylene chains for hydrophilicity.[2–5] They can form micelle in aqueous phase where the nucleation of the latex particles primarily occurs. The main factor affecting the emulsion stability is the length of the hydrophilic chain. The increasing of the length of the hydrophilic chain results in an increase in the colloidal stability of the polymerization system via the steric stabilization effect.

In addition, a few publications[6–8] dealt with the mechanism of the stabilization of alkali soluble random copolymers as a polymeric surfactant in emulsion. This kind of copolymers is an ionic polymeric surfactant and contains both hydrophobic chains and a large number of carboxyl groups which can stabilize polymer particles by the electrostatic effect. The carboxyl content in the copolymers plays an important role in the stability of emulsion, polymerization rate, viscosity of emulsion, and the morphology of the final latex. The molecular weight distribution of the copolymers influences the latex particle size distribution. Though the general structure of ionic random copolymers is similar to that of conventional emulsifiers, the behavior of ionic random

Correspondence to: F.-Q. Liu (liufengqi@jlu.edu.cn).

copolymers in emulsion polymerization and their contribution to emulsion polymerization would be different from those of conventional emulsifiers.

Butyl acrylate is perhaps the most important acrylic monomer in terms of application. It is a good component for paints, adhesives, etc. In the present study, a polymeric surfactant based on butyl acrylate was prepared and its role in the emulsion polymerizations of styrene was investigated with the hope that the polymeric surfactant stabilized latex would be applied in the paint and coating industries in the future.

EXPERIMENTAL

Materials

All the materials were obtained from the Tianjin Tiantai Chemical Reagent Co. Butyl acrylate (BA) and styrene (St) monomer were distilled under reduced pressure before use. Maleic anhydride (MAH) and benzoyl peroxide (BPO) were purified by recrystallization in chloroform. Potassium persulfate (KPS) was purified by recrystallization in deionized water. Tetrahydrofuran (THF) was dried by refluxing with metallic sodium followed by distillation. Chloroform, methanol, sodium bicarbonate ($NaHCO_3$), and sodium hydroxide (NaOH) were all analytical grade and used as received. Distilled water was applied in all emulsion polymerizations.

Preparation of the amphiphilic random copolymer

First, P (BA-co-MAH) was prepared by solution copolymerization of BA and MAH. In a 500 mL reactor, MAH (0.3 mol) and BPO (6×10^{-4} mol) were dissolved in THF (200 mL) and the solution was deoxygenated with nitrogen. BA (0.3 mol) was added dropwise to the solution when the temperature reached 60°C. The polymerization was carried out at 60°C under nitrogen atmosphere for 24 h. The polymerization product was precipitated in methanol three times and dried in a vacuum oven at room temperature. Second, P (BA-co-MAH) was hydrolyzed in a 1 mol/L aqueous solution of sodium hydroxide at 50°C. This condition was chosen so as to avoid the hydrolysis of ester groups in the copolymer. The reaction product was purified with ethanol as precipitation agent and dried in an oven at 50°C and an amphiphilic random copolymer was obtained.

Characterization of the amphiphilic random copolymer

FTIR spectrum of the amphiphilic random copolymer was recorded with infrared spectrophotometer (Vector 22 FT-IR, Bruker, Germany) and ^1H NMR spectrum was recorded with an Ultrashield spectrometer (500 MHz, Bruker, Germany) using $CDCl_3$ as solvent at ambient temperature. Based on the integral area of proton signals of methyl groups ($A_{\delta\,=\,0.935} = 1$), the molar ratio of BA to MAH (x/y) was calculated by means of the following equation:

$$\frac{x}{y} = \frac{\frac{A_{\delta\,=\,0.935}}{3}}{\frac{A_{\text{total}} - A_{\text{BA}}}{2}} \quad (1)$$

where $A_{\delta=0.935}$ is the integral area of proton signals of methyl groups, A_{total} is the integral area of proton signals of copolymer, A_{BA} is the integral area of proton signals of BA component and it is four times of $A_{\delta=0.935}$.

The method of surface tension was used to determine the CMC of the amphiphilic random copolymer. Steps were as follows. The amphiphilic random copolymer was dissolved in distilled deinonized water to prepare a 5% solution, which was then serially diluted. Wilhelmy plate method using a standardized plate with a plate tensiometer (BYZ-1, Shanghai, China) was used to measure the surface tension of the solution.

Emulsion polymerization process

Emulsion polymerization was carried out in a 250 mL reactor equipped with an agitator, a nitrogen inlet tube, and a reflux condenser. The water/styrene weight radio (10 : 1) was constant for all the experiments. A typical procedure could be briefly described as follows. First, a mixture composed of water, monomer, a prescribed amount of amphiphilic random copolymer and sodium bicarbonate (buffer) was charged into the reactor and dispersed by ultrasonication (KQ-200VDB, 45 kHz, 100 W, Kunshan, China) for 20 min. Then the reaction system was purged with nitrogen for the removal of oxygen, and heated to the polymerization temperature. This was followed by the addition of a prescribed amount of initiator solution consisting of potassium persulphate and water to the reactor to start the polymerization. The temperature fluctuation was controlled within a range of ± 0.5°C, and the agitation speed was kept constant at 200 rpm throughout the reaction. The basic recipe is listed in Table I.

Latex characterization

Conversion

The conversion of St (X) was determined gravimetrically. Aliquots of about 1 to 2 g were withdrawn with a syringe at appropriate intervals and poured into a weighed small aluminium foil dish. To prevent monomer from further polymerization, a drop of aqueous solution of hydroquinone at 1 wt % was added to the sample. Monomer and water were driven off by drying to constant weight in a vacuum

TABLE I
Basic Recipe of Emulsion Polymerization

Runs	[St] (g/mL)	H_2O (mL)	[S][a] (g/L)	[KPS][b] (mM)	[$NaHCO_3$][c] (mM)	T (K)
A	0.1	50	16	3.70	11.9	343
B	0.1	50	8	3.70	11.9	343
C	0.1	50	4	3.70	11.9	343
D	0.1	50	2	3.70	11.9	343
E	0.1	50	8	3.70	11.9	343
F	0.1	50	8	2.96	9.52	343
G	0.1	50	8	2.22	7.14	343
H	0.1	50	8	1.85	5.95	343
I	0.1	50	8	1.66	5.35	343
J	0.1	50	8	1.48	4.76	343
K	0.1	50	8	1.11	3.57	343
L	0.1	50	8	3.70	11.9	348
M	0.1	50	8	3.70	11.9	343
N	0.1	50	8	3.70	11.9	338
O	0.1	50	8	3.70	11.9	333

[a] In Runs B, E, and M, the standard deviation of [S] is ±0.005.
[b] In Runs B, E, and M, the standard deviation of [KPS] is ±0.0003.
[c] In Runs B, E, and M, the standard deviation of [NaHCO3] is ±0.009.

oven at 60°C. The dried sample was weighed to calculate monomer conversion based on the following equation:

$$X(\%) = \frac{m_{ds}/m_s - w_c}{w_m} \times 100\% \quad (2)$$

where m_{ds} is the mass of dried sample (g), m_s is the mass of sample (g), w_c is the mass fraction of nonpolymeric solid, and w_m is the initial mass fraction of the monomer.

On the assumption that the monomer is entirely in the monomer droplets or particles, the polymerization rate R_P versus conversion curves were obtained by the graphic method and R_P was calculated as follows:

$$R_P = [M]_0 \cdot \frac{dx}{dt} \quad (3)$$

where R_P is the rate of polymerization (mol/L s), $[M]_0$ is the initial concentration of the monomer in the reactor (mol/L), x is the fractional conversion and $\frac{dx}{dt}$ is the slope of x-t curve at any point.

Particle size

Dynamic light scattering (DLS; Zeta Plus Zeta Potential Analyzer, Brookhaven Instruments Co., USA) was used for monomer drop and latex particle size measurement. Sample preparation was carried out according to the following procedure. The emulsion dispersed by ultrasonication and the latex product were diluted with filtered and distilled water to an appropriate concentration (Avg. Count Rate: 200-800 kcps) respectively, and then measured in the instrument. Particle's size and their shape for some final latex were also measured via a transmission electron microscope (TEM; Hitachih-8100, Japan). At least 300 latex particles per sample were counted in the particle size measurement. From the TEM analysis volume average particle diameter (D_V) was calculated by means of the following equation.

$$D_v = \left[\frac{\sum_{n_i} \cdot D_i^3}{\sum_{n_i}}\right]^{1/3} \quad (4)$$

Number of particles

On the basis of the D_V data, the number of monomer droplets per liter of water immediately before the start of polymerization ($N_{m,\,i}$) and the number of latex particles per liter of water produced at the end of the emulsion polymerization ($N_{P,\,f}$) was calculated from the following equation.[8]

$$N_{m,i} = \frac{6 \cdot M_{mw}}{\pi \rho_m \cdot {D_V}^3} \quad (5)$$

$$N_{P,f} = \frac{6 \cdot M_{mw} \cdot x}{\pi \rho_p \cdot {D_V}^3} \quad (6)$$

where M_{mw} is the initial monomer-to-water ratio (g/mL), x is the fractional conversion, ρ_m is the monomer density (g/mL), ρ_p is the polymer density (g/mL), and D_V is volume average diameter (cm).

Estimation of average number of radicals per particle ($\bar{n}$)

From the experimental values of R_P and N_P (particle number), the literature values of the propagation

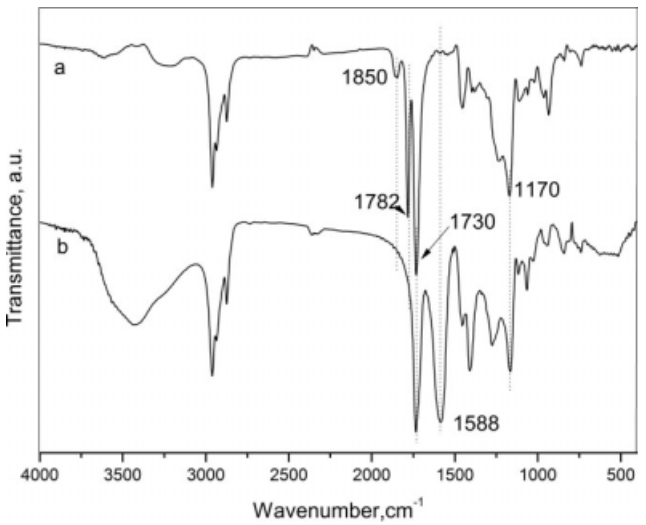

Figure 1 FT-IR spectrum of P (BA-co-MAH) (a) and P (BA-co-MANa) (b).

rate constant ($k_p = 4.27 \times 10^7 \exp[-32{,}510/RT]$ $dm^3mol^{-1}s^{-1}$)[13] and the equilibrium styrene monomer concentration in the PSt particles ($[St]_p = 5.2$ mol dm^{-3}),[14] $\overline{n}$ was estimated from the following aquation[15]:

$$R_P = \frac{k_p[St]_p N_p \overline{n}}{N_A} \quad (7)$$

where N_A is the Avogadro's number, R is the gas constant (8.314 J/mol K), and T is the absolute temperature (K).

RESULTS AND DISCUSSION

Characterization of the amphiphilic random copolymer

Figure 1 shows the typical IR spectra of copolymer P (BA-co-MAH) and its hydrolysate P (BA-co-MANa) (the amphiphilic random copolymer). It testifies that the hydrolysis reaction was very efficient. The spectrum of the former shows the characteristic anhydride peaks at ca. 1782 cm^{-1} and 1850 cm^{-1}, ester carbonyl peak at 1730 cm^{-1}, and ether peak at 1170 cm^{-1}, respectively. In the spectrum of the latter (the amphiphilic random copolymer), the anhydride peaks have disappeared and instead the spectrum shows characteristic absorption of carboxylic acid salt at 1589 cm^{-1}. The ether peak at 1170 cm^{-1} has not changed, indicating that the ester hydrolysis did not take place.

^{1}H NMR spectrum of P (BA-co-MAH) is shown in Figure 2. The main peaks are clearly identified in this Figure. According to eq. (1), the BA molar content in P (BA-co-MAH) was 63.5%. The BA molar content in P (BA-co-MANa) was considered to be the same as that of P (BA-co-MAH). Scheme 1 shows the structures of P (BA-co-MAH) and P (BA-co-MANa).

The CMC of P (BA-co-MANa) measured via surface tension was 7.09 g/L. Compared with that of similar polymeric surfactant (e.g. ASR),[6] the CMC value was higher. The possible reason was that the hydrophilicity of P (BA-co-MANa) was better because of the existence of dicarboxyl group.

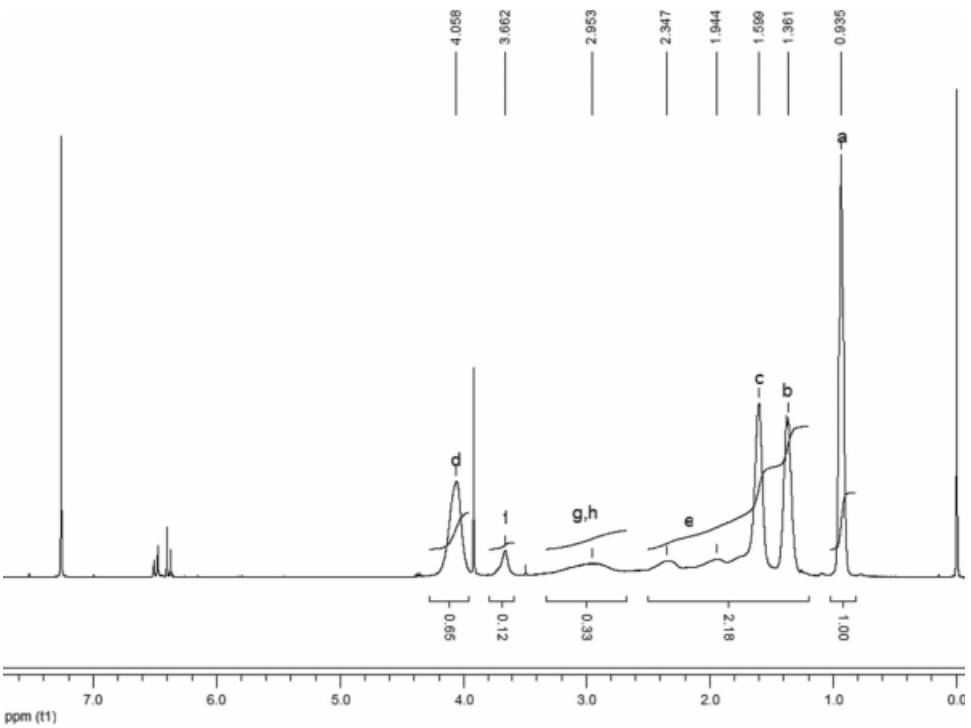

Figure 2 ^{1}H NMR spectrum of P (BA-co-MAH).

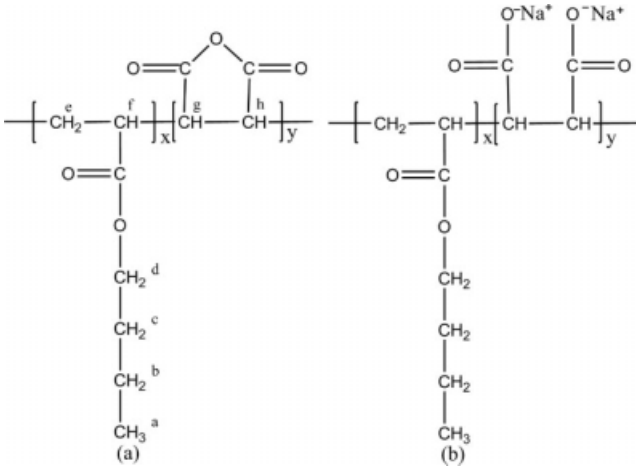

Scheme 1 Molecular structure of P (BA-co-MAH) (a) and P (BA-co-MANa) (b).

Effect of polymeric surfactant concentration

In this series of experiments (Runs A-D), the amphiphilic random copolymer with four different concentrations were used as polymeric surfactant to stabilize the emulsion polymerization of styrene. The profiles of reaction time (t) versus monomer conversion (X) and X versus R_P (inset) for St emulsion polymerizations stabilized by polymeric surfactant with various [S] are shown in Figure 3. Some experimental data obtained from the polymerizations stabilized by polymeric surfactant are listed in Table II. It is shown that the final conversion increased with the increasing of [S]. In Runs A, B, and C, the final conversion could reach more than 95%, whereas in Run D, a conversion of 86% was only achieved within 1 h, and the stability of the polymeric surfactant to the latex particles was poor (Total scrap is 6.37%).

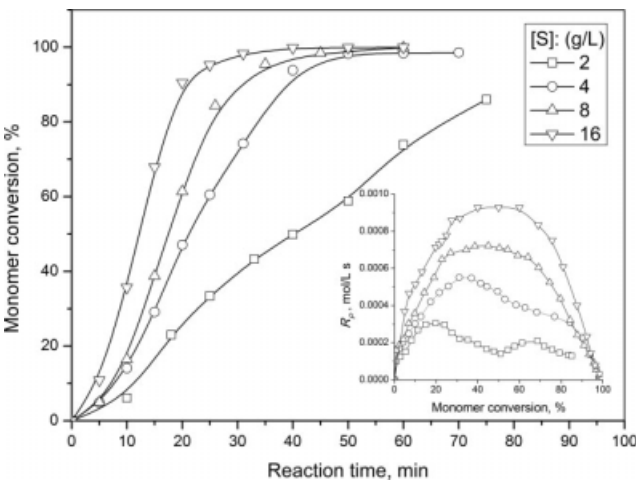

Figure 3 Variation of the monomer conversion (X) with the reaction time (t) at different [S] (the inset shows R_P versus X plots).

TABLE II
Some Experimental Data Obtained From Styrene Emulsion Polymerization at Various [S]

	A	B	C	D
[S] (g/L of H_2O)	16	8	4	2
$R_P \times 10^4$ (mol/L s)	9.28	7.20	5.48	3.00
$D_{DLS,m,i}$ (nm)[a]	46.4	52.8	96.6	197.2
$D_{DLS,p,f}$ (nm)[b]	83.8	88.6	155.2	223.5
$N_{DLS,m,i} \times 10^{-17}$ (1/L)[c]	18.0	12.2	2.00	0.24
$N_{DLS,p,f} \times 10^{-17}$ (1/L)[d]	3.06	2.59	0.47	0.14
$N_{DLS,p,f}/N_{DLS,m,i}$	0.17	0.21	0.24	0.58
$D_{TEM,p,f}$ (nm)[e]	—	46.0	62.2	90.4
$N_{TEM,p,f} \times 10^{-17}$ (1/L)[f]	—	18.5	7.4	2.1
$\bar{n}$	—	0.09	0.18	0.34
Total scrap (%)	0.03	0.09	1.44	6.37

[a] The average monomer droplet size immediately before the start of polymerization by DLS method.
[b] The average size of the resultant latex particles by DLS method.
[c] The number of monomer droplets per liter water produced immediately before the start of polymerization by DLS method.
[d] The number of latex particles per liter water formed at the end of polymerization by DLS method.
[e] The average size of the resultant latex particles by TEM method.
[f] The number of latex particles per liter water formed at the end of polymerization by TEM method.

The inset plots in Figure 3 show how the maximal rate of polymerization increased with the increasing of [S]. This trend that the maximal rate of polymerization increased with the increasing of [S] was attributed to an increased the number of active sites (or particles) with [S]. The variation of R_P with different [S] presented two cases. When [S] was above its CMC (Runs A and B), R_P increased to the primary maximum, followed by a decrease. The polymerization lied in a clear constant rate interval (Interval II). It would be discussed later whether the polymerization follows Smith-Ewart Case II kinetics or not. When [S] was lower than its CMC (Runs C and D), a constant rate interval was not apparent. Besides, there was the second increasing of R_P in the higher conversion. The lower [S] was, the more obvious the second increasing of R_P was.

Chern et al.[5] indicated that apparently Smith-Ewart Case II kinetics was not applied to the polymerization system with PEG-containing graft copolymers as the steric stabilizers. According to the micelle nucleation theory,[16,17] latex particles are generated via the capture of free radicals by micelle in emulsion polymerization. Furthermore, Smith-Ewart Case II kinetics predicts that both R_P and N_P are proportional to the 0.6th power of [S] and 0.4th powers of initiator concentration ([I]), respectively. However, in the present system, the fitted exponents of Smith-Ewart relationships ($R_P \propto [S]^{\alpha}$ and $N_P \propto [S]^{\beta}$) obtained from polymerization with various [S]

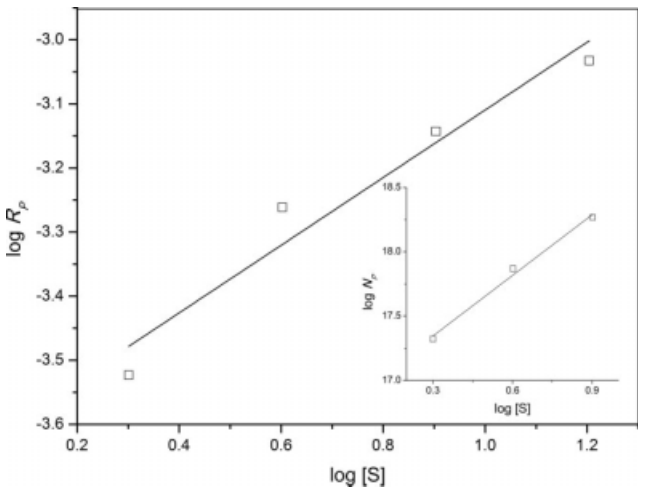

Figure 4 Relationship between R_P and [S] in logarithm (the inset is relationship between N_P and [S] in logarithm).

are $\alpha = 0.53$ and $\beta = 1.57$, respectively (Fig. 4). Although the relationship of R_P with [S] is similar to the micelle nucleation model ($\alpha = 0.6$), the relationship of N_P with [S] strongly deviates from the micelle nucleation model ($\beta = 0.6$). Similar behavior was discussed in terms of the oil solubility of a nonionic emulsifier.[18,19] Introducing the concept of the effective concentration of surfactant could interpret this deviation. Because of the high oil solubility of polymeric surfactant, the amount of surfactant playing an effective role in emulsification is much less than the total amount surfactant used, which supports the pseudobulk kinetics or increasing importance of the particle volume in the emulsion polymerization of St stabilized by the polymeric surfactant. Another reason might be that the mixed mode of particle nucleation consists in emulsion polymerization. As the mechanical agitator cannot make the reactant form homogenized emulsion in lower surfactant concentration, the method of ultrasonic emulsification is used. The monomer is dispersed to small droplets by high-energy ultrasonic (Table II). The small droplets have the ability of capturing free radicals, so the droplets nucleation[20,21] and micelle nucleation might coexist in the polymerization system.

When [S] is higher than CMC (Runs A and B), the polymeric surfactant could form micelle in aqueous phase. Because small monomer droplets and the monomer-swollen micelles can capture free radical to form latex particles, it is obvious that two forms of nucleation coexist in polymerization. In the classical emulsion polymerization of hydrophobic monomer (e.g. St), the stage of forming nucleation (Interval I) is very short and ends at X = 5–10%. In our system, the numbers of reaction loci increase up to ca. 35% conversion. With the increasing of [S], the stage of forming nucleation (Interval I) is longer (Run A, X = ca. 0–40%, and Run B, X = ca. 0–35%). This is the result of the decreasing of the entry coefficient of radicals (this is discussed later). The latex particles (N_P) would not increase after the polymeric micelle have been exhausted, which is then followed by a stage with a constant R_P (X = ca. 40–60%). After the constant R_P has been achieved, the decrease in R_P with X is attributed mainly to the decrease of the monomer concentration. When [S] is lower than CMC (Runs C and D), the droplets nucleation becomes the main model of latex generation because of the lack of micelle and a clear constant rate interval (interval II) could not be found. The polymeric surfactant as stabilizer and costabilizer restrain the fusion of small droplets (Ostwald ripening).[4,22] The appearance of the second maximal rate at a high conversion ($X > 60\%$) is related closely to the accumulation of radicals within the polymer particles. This is gel effect (pseudobulk kinetics). As the polymerization advances, the monomer concentration in the particles decreases, therefore, the viscosity within the particles increases significantly. The accumulation of radicals in the particles caused by the decreased bimolecular termination rate leads to the gel effect and the increasing of R_P.

According to the eq. (7), the average Number of Radicals per Particle ($\overline{n}$) was calculated with different [S]. The value of $\overline{n}$ was less than 0.5 in all the runs, and it decreased with the increasing of [S] (Table II). Because $R_P = k_p$ [St]$_p$ ($\overline{n}N_P/N_A$) and $\overline{n}$ did not remain constants for the systems with different [S], the relationship of N_P and R_P was not a simple linear correlation. This is consistent with the result that the exponent α was not equal to β. The polymeric surfactant was composed of a large number of hydrophobic segments and a relatively small quantity of carboxyl groups. When the surfaces of particles were covered with large number of the polymeric surfactant, the polymeric surfactants could create a strongly viscous region around the particles. The region not only reduced the coalescence of droplets considerably, but also prevented free radicals from being adsorbed onto and entering into the monomer droplets because of their interfacial rigidity.[6,23] So $\overline{n}$ was less than 0.5. The $\overline{n}$ value increased with particle size only because more radicals could be accommodated within the large latex particle and the probability of radicals to be transported out of latex particles decreased.

To understand the effect of [S] on particle size, DLS was adopted to measure the average monomer droplet size before polymerization ($D_{\mathrm{DLS,m,i}}$) and the average size of the resultant latex particles ($D_{\mathrm{DLS,p,f}}$). The relevant numbers of particles ($N_{\mathrm{DLS,m,i}}$, $N_{\mathrm{DLS,p,f}}$) were calculated by means of eqs. (5) and (6). The data show that $D_{\mathrm{DLS,m,i}}$ and $D_{\mathrm{DLS,p,f}}$ increased with the decreasing of [S]. The reason was that the

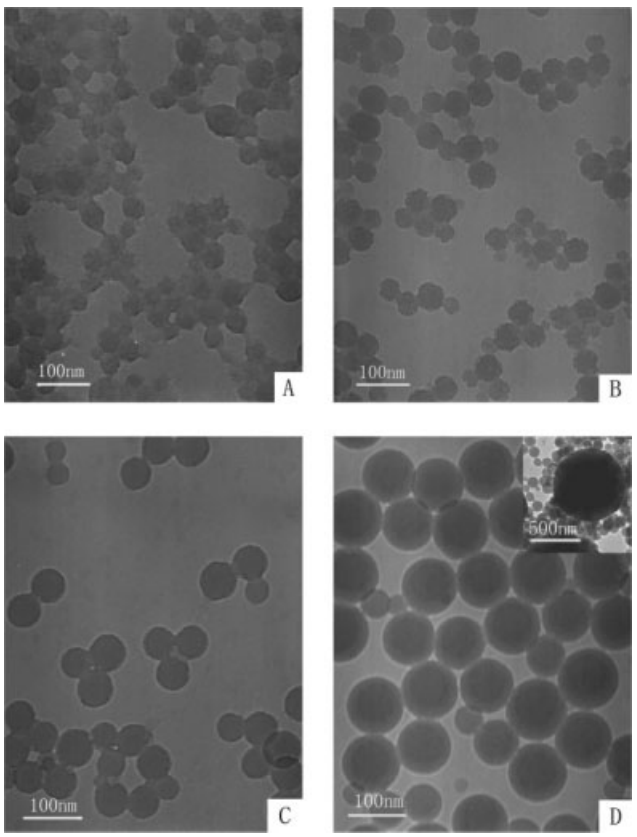

Figure 5 TEM images of final polystyrene latex particles prepared with various [S]: (A) [S]: 16 g/L; (B) [S]: 8 g/L; (C) [S]: 4 g/L; (D) [S]: 2 g/L (the inset shows the contrast between small particles and large particles).

increasing of particle diameter could decrease its surface area, which made the less amount of the surfactant sufficiently cover the surface of particles. In addition, $N_{DLS,p,f}/N_{DLS,m,i} < 1$ and the ratio decreased with the increasing of [S], i.e., $N_{DLS,p,f}$ was not equal to $N_{DLS,m,i.}$ This deviated the mechanism of miniemulsion polymerization (the number of the nucleated particles was constant during the polymerization). The reason might be that the fusion of small droplets (Ostwald ripening)[24,25] could not be restrained effectively by polymeric surfactant. It might also be that the conglutination or the coalescence occurred to latex particles. The conglutination phenomenon of particles was confirmed by the TEM photographs (Fig. 5).

The representative transmission electron micrograph of final polystyrene latex is shown in Figure 5. It could be observed that the spherical latex particles with two different size distributions were formed at [S] = 2 g/L. One was at ca. 100 nm and the other was at ca. 500 nm. Moreover, the number of small particles was more and their distribution was more uniform. The formation of large particles might be due to that lower surfactant concentration could not stabilize latex particles well, so that the

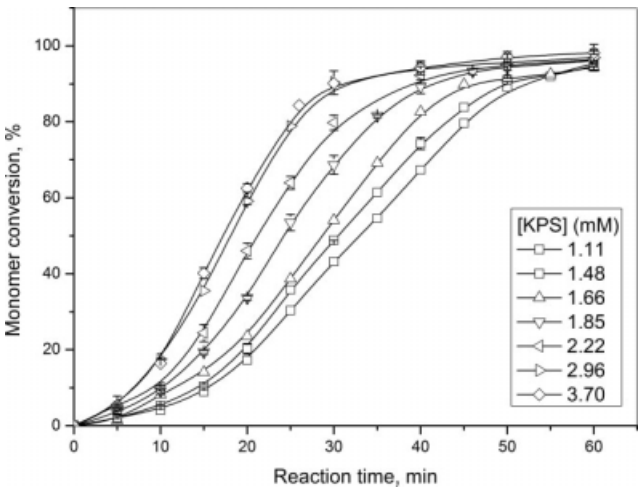

Figure 6 Variation of the monomer conversion (X) with the reaction time (t) at different [KPS].

coalescence of latex particle occurred in the later stage of reaction. With the increase of [S], the shape and size of latex particles gradually became irregular. As [S] was up to 16 g/L, the formed latex particles conglutinated together. However, this did not affect the stability of emulsion. It could also be proved very well by the total scrap of 0.03%. According to experimental result, the conglutination between latex particles was different from the coalescence of particles. In emulsion polymerization, the appearance of coalescence meant the reducing of active centers and the decreasing of R_P. However, R_P increased with increasing of [S] and was not influenced by high conglutination. It proved that the number of active centers did not change and only form a kind of large heterogeneous particles with multiple-active-sites. The original small particles were separated from one another by the polymeric surfactant layer, which depressed the diffusion of

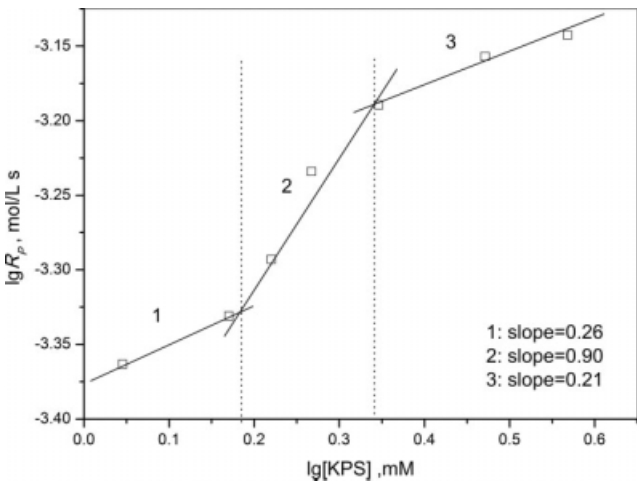

Figure 7 Relationship between R_P and [KPS] in logarithm.

TABLE III
R_P Obtained From Styrene Emulsion Polymerization at Various [KPS]

	E	F	G	H	I	J	K
[KPS] (mM)	3.70	2.96	2.22	1.85	1.66	1.48	1.11
$R_P \times 10^4$ (mol/L s)	7.20	6.97	6.47	5.83	5.09	4.67	4.33

radicals within such a heterogeneous particle. The higher the [S] was, the more severe the conglutination was. The existence of plentiful surfactant among particles stabilized the emulsion well. It could also prove that the emulsion was stabilized by steric stabilization effects in addition to the static repulsion of the charges of surfactant themselves. This made $D_{DLS,p,f} > D_{TEM,p,f}$ listed in Table II. The further research is required to clarify why the conglutination of latexes increased with increasing of [S].

Effect of initiator concentration

In this series of experiments (Runs E-K), [S] was kept constant and the initiator concentration ([KPS]) was varied from 1.11 to 3.70 mM. Figure 6 shows X versus t profiles at different [KPS]. As expected, the overall polymerization rate increased with increasing amounts of initiator. It is because the number of the nucleated particles increases with increasing [KPS]. But the relationship of R_P ($[M_0]$ dx/dt) with [KPS] presented obviously different (Fig. 7 and R_P data in Table III), dx/dt was determined from the linear portion of the x-t curve in Figure 6. When [KPS] was lower than 1.53 mM or higher than 2.19 mM, R_P increased slowly with the increasing of [KPS]. But R_P increased markedly when [KPS] increased from 1.53 to 2.19 mM. The following relationships hold: $R_P \propto [KPS]^{0.26}$ for [KPS] $<$ 1.53 mM, $R_P \propto [KPS]^{0.90}$ for [KPS] being between 1.53 and 2.19 mM, and $R_P \propto [KPS]^{0.21}$ for [KPS] $>$2.19 mM. A possible reason for these observations could be as follows: The presence of the polymeric surfactant which created a viscous region around the particles resulted in a decrease in the diffusion rate of free radicals. As [S] was constant, the concentration of decomposed radicals around each monomer drop increased with the increasing of [KPS]. At lower [KPS] ([KPS] $<$ 1.53 mM), the primary radical formed in the aqueous phase was little and held up by the viscous region around the monomer droplets (or the monomer-swollen micelles). The barrier to make radicals difficult to enter into monomer droplets influenced the increased rate of R_P with increasing [KPS]. The exponent 0.26 in the relationship $R_P \propto [KPS]^{0.26}$ was gained by linear fitted (stage 1 in Fig. 7) and R_P was mainly controlled by the barrier effect. With the increasing of [KPS], the probability of radicals to enter into monomer droplets was increased. When [KPS] increased to an appropriate concentration (between 1.53 and 2.19 mM), the probability that two active radicals entered simultaneously into a latex particle was diminished, the lifetime of an oligomeric radical in active particle would be prolonged, and the influence of increasing [KPS] on R_P was prominent. It was attributed to restricted termination of the radicals owing to the barrier effect of the polymeric surfactant region. When the exponent was 0.90 in the relationship $R_P \propto [KPS]^{0.90}$ (stage 2 in Fig. 7), R_P was mainly controlled by the restricted termination. When [KPS] was higher than 2.19 mM, the probability of several active radicals entering simultaneously into a latex particle was increased. Therefore, the bimolecular termination restrained the increasing of R_P with the increasing [KPS]. For the case of exponent 0.21 in the relationship $R_P \propto [KPS]^{0.21}$ (stage 3 in Fig. 7), R_P was mainly controlled by the dimolecular termination.

Effect of polymerization temperature

In this series of experiments (Runs L-O), the reaction temperature (T) varied from 60°C to 75°C. Figure 8 showed the profiles of X versus t for polymerizations carried out at different temperatures. With increasing of T, R_P (constant polymerization rate, Table IV) increased because the overall polymerization rate constant (k) increased significantly (Table IV). If the radical desorption was ignored, k is equal to $k_p(k_d/k_t)^{1/2}$, k_p is the propagation rate constant, $k_d = 6.06 \times 10^{16} \exp(-14{,}0167/RT)$[26] is the initiator

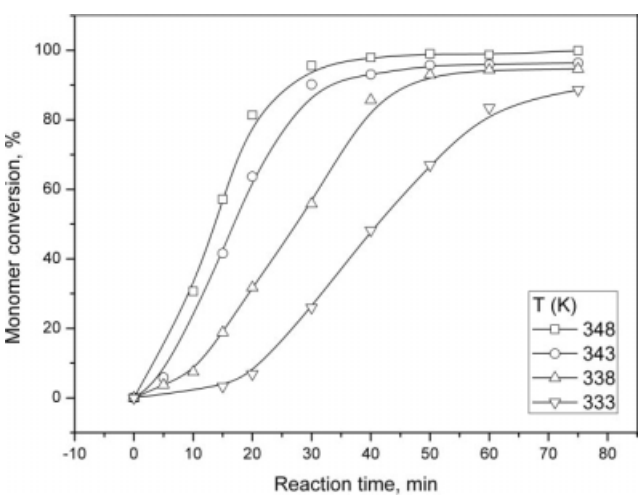

Figure 8 Variation of the monomer conversion (X) with the reaction time (t) at different reaction temperature (T).

TABLE IV
R_P and the Overall Polymerization Rate Constant (k) Obtained From Styrene Emulsion Polymerization at Various T

	I	J	K	L
T (K)	348	343	338	333
$R_P \times 10^4$ (mol/L s)	7.88	7.20	3.93	3.40
$k \times 10^4$ (L/mol s^2)$^{1/2}$	5.68	3.51	2.14	1.29

decomposition rate constant, and $k_t = 8.2 \times 10^9 \exp(-14{,}510/RT)$[27] is the termination rate constant. Therefore, the increasing of R_P with increasing the temperature was the result of a combination of three factors (decomposition, propagation, and termination). Among them, the initiator decomposition rate was the most important factor. In fact, the transport of radicals out of latex particles was inevitable in emulsion polymerization and this would reduce $\bar{n}$ and, therefore, decrease R_P. This desorption phenomenon would decrease the overall activation energy of the reaction. Based on the data of R_P and T, the polymerization reaction activation energy obtained from the Arrhenius equation was 60.29 kJ/mol.

CONCLUSION

In this work, a polymeric surfactant was prepared and characterized. The molar radio of BA and MANa in the polymeric surfactant was 63.5 : 36.5 via the characterization of ^{1}HNMR. The CMC of the polymeric surfactant measured via surface tension was 7.09 g/L. The mechanism of particles nucleation and the effectiveness of the polymeric surfactant in stabilizing styrene emulsion polymerization were evaluated. R_P increases with the increasing of [S]. The second maximum was attributed to the gel effect at a lower [S]. The contribution of small monomer droplets to the whole particle nucleation mechanism process would be primary and micelle nucleation could not be ruled out at a higher [S]. R_P and N_P generated are approximately proportional to the 0.53th and 1.57th powers of the total [S], respectively. The average number of radicals per particle is less than 0.5 and it is inversely proportional to the surfactant concentration. There was the phenomenon that latex particles conglutinated to a kind of special particle with multiple-active-sites during polymerization and the conglutination became severe with the increase of the polymeric surfactant concentration. The influence of the initiator concentration on polymerization rate was complex. When the initiator concentration was between 1.53 and 2.19 mM, the sensitivity of R_P to the variation of the initiator concentration was high. When the initiator concentration was lower than 1.53 mM or higher than 2.19 mM, the variation of R_P with the initiator concentration was slight. R_P increased with increasing of T, the activation energy in polymerization of styrene stabilized by polymeric surfactant was calculated to be 60.29 kJ/mol.

References

1. Wang, X.; Sudol, E. D.; El-Aasser, M. S. Macromolecules 2001, 34, 7715.
2. Piirma, I.; Lenzotti, J. R. Br Polym J 1989, 21, 45.
3. Jialanella, G. L.; Firer, E. M.; Piirma, I. J Polym Sci Part A Polym Chem 1992, 30, 1925.
4. Chern, C. S.; Lee, C. Macromol Chem Phys 2001, 202, 2750.
5. Chern, C. S.; Lee, C. J Polym Sci Part A Polym Chem 2002, 40, 1608.
6. Lee, D. Y.; Kim, J. H. J Polym Sci Part A Polym Chem 1998, 36, 2865.
7. Wang, S. J.; Qiang, Y.; Zhang, Z. C. Colloids Surf A 2006, 281, 156.
8. Wang, S. J.; Qiang, Y.; Zhang, Z. C. Eur Polym J 2007, 43, 178.
9. Maria, E.; Rotureau, E.; Dellacherie, E.; Durand, A. Colloids Surf A 2007, 308, 25.
10. Cheong, I. W.; Nomra, M.; Kim, J. H. Macromol Chem Phys 2001, 202, 2454.
11. Zhang, J. Z.; Cao, Y.; He, Y. H. J Appl Polym Sci 2004, 94, 763.
12. Zhang, Q. Y.; Lee, D. Y.; Cheong, I. W.; Shin, J. S.; Park, Y. J.; Kim, J. H. J Appl Polym Sci 2003, 87, 1941.
13. Gilbert, R. G. Pure Appl Chem 1996, 68, 1491.
14. Barthalome, E.; Gerrens, H.; Herbeck, R.; Weitz, H. M. Z Elektrochem 1956, 60, 334.
15. Smith, W. V.; Ewart, R. H. J Chem Phys 1948, 16, 592.
16. Harkins, W. D. J Am Chem Soc 1947, 69, 1428.
17. Smith, W. V. J Am Chem Soc 1948, 70, 3695.
18. Capek, I.; Barton, J.; Tuan, L. Q.; Svoboda, V.; Novotny, V. Makromol Chem 1987, 188, 1723.
19. Piirma, I.; Chang, M. J Polym Sci Polym Chem Ed 1982, 20, 489.
20. Ugelstad, J.; El-Aasser, M. S.; Vanderhoff, J. W. J Polym Sci Polym Lett Ed 1973, 11, 503.
21. Ugelstad, J.; Hansen, F. K.; Lange, S. Makromol Chem 1974, 175, 507.
22. Miller, C. M.; Sudol, E. D.; Silebi, C. A.; El-Aasser, M. S. Macromolecules 1995, 28, 2754.
23. Coen, E. M.; Lyons, R. A.; Gilbert, R. G. Macromolecules 1996, 29, 5128.
24. Mishchuk, N. A.; Verbich, S. V.; Dukhin, S. S. J Dispersion Sci Techn 1997, 18, 517.
25. Kabalnov, A. S.; Shchukin, E. D. Adv Colloid Interface Sci 1992, 38, 69.
26. Kolthoff, I. M.; Miller, I. K. J Am Chem Soc 1951, 73, 3055.
27. Matheson, M. S.; Auer, E. E.; Bevilacqua, E. B.; Hart, E. J. J Am Chem Soc 1951, 73, 1700.